Measurement of the Full Refractive Index Tensor in Sheared Liquid Crystalline Polymer Solutions

K. Hongladarom and W. R. Burghardt*

Department of Chemical Engineering, Northwestern University, Evanston, Illinois 60208

Received September 3, 1993; Revised Manuscript Received October 25, 1993•

ABSTRACT: The full refractive index tensor of sheared liquid crystalline solutions of poly(γ-benzyl glutamate) in *m*-cresol has been measured using a combination of optical techniques. At all shear rates studied, the average molecular orientation direction is within 2 deg of the flow direction. In the low shear rate tumbling regime, the orientation angle is positive, in agreement with the Larson–Doi polydomain model [Larson, R. G.; Doi, M. *J. Rheol.* **1991**, *35*, 539]. As shear rate is increased, the orientation angle changes sign, consistent with a transition from tumbling to flow alignment, as predicted by the Doi molecular model [Marrucci, G.; Maffettone, P. L. *Macromolecules* **1989**, *22*, 4076. Larson, R. G. *Macromolecules* **1990**, *23*, 3983]. This transition appears to be shifted to higher shear rates at higher concentrations. The low shear rate regime is characterized by a biaxial average refractive index tensor, with enhanced molecular orientation along the vorticity direction relative to the shear gradient direction. This is in qualitative agreement with the Larson–Doi model, which however underpredicts the misalignment of domains, both within and out of the flow–vorticity plane. At high shear rates, the average refractive index tensor is approximately uniaxial. Long after cessation of shear flow at a low rate, the resulting high orientation state is uniaxial but is characterized by a *negative* orientation angle when the previous shear rate is in the low shear rate, tumbling regime. This indicates that the average orientation direction changes sign during relaxation under these conditions.

1. Introduction

The technological applications of liquid crystalline polymers depend on the ability to influence their microscopic structure during processing, through applied deformation. The past decade has consequently seen numerous experimental and theoretical studies of the rheological behavior and structure of liquid crystalline polymers. Recently, some of these efforts have focused on a detailed characterization of the molecular orientation state of textured liquid crystalline polymers under shear, at both microscopic[1–7] and averaged macroscopic[6–9] levels. In the latter vein, we have recently published a study of average molecular orientation in textured solutions of poly(γ-benzyl glutamate) [PBG] in *m*-cresol under shear, using birefringence.[10,11] This work had two distinguishing characteristics. First, a spectrographic birefringence technique was employed, eliminating ambiguities associated with multiple retardation orders and allowing a quantitative measure of molecular orientation. Second, by measuring the birefringence of quiescent PBG monodomains, we were able to quantify the degree of disruption in molecular orientation associated with shear flow, enabling tests of available theories in considerable detail.

All of the studies of average molecular orientation in PLC's published to date have measured only one projection of the orientation state. For example, flow birefringence measures optical anisotropy in the plane perpendicular to the light propagation direction. In the case of applied shear flow in the "1" direction, with velocity gradient in the "2" direction, symmetry arguments dictate that the anisotropic part of the refractive index tensor will take the form

$$\mathbf{n} = \begin{bmatrix} n_{11} & n_{12} & 0 \\ n_{12} & n_{22} & 0 \\ 0 & 0 & n_{33} \end{bmatrix} \tag{1}$$

By analogy with the stress tensor in shear flow, we recognize that $\mathbf{n}$ may be fully characterized by three independent quantities, which could be chosen as the shear component, n_{12}, and two normal "optical" differences $\Delta_1 = n_{11} - n_{22}$ and $\Delta_2 = n_{22} - n_{33}$. As an alternative to specifying the shear component, we can define the optical orientation angle in the shear plane:

$$\chi = \frac{1}{2}\tan^{-1}\left(\frac{2n_{12}}{\Delta_1}\right) \tag{2}$$

In our prior work,[10,11] the light beam passed through the shear flow along the "2" axis, allowing for measurement of anisotropy in the 1–3 plane, such that the measured birefringence $\Delta n = n_{11} - n_{33} \equiv \Delta_3$. Here Δ_3, the third normal optical difference equals the sum of Δ_1 and Δ_2. Thus, these measurements were insensitive to, for instance, the orientation angle within the shear plane. Similarly, small angle X-ray scattering studies of molecular orientation have typically used a beam parallel to the gradient direction as well, so that they also probe orientation in the 1–3 plane.[6–8]

In order to determine the optical orientation angle, it is common practice in flow birefringence to sample an alternate projection of $\mathbf{n}$ by sending light down the vorticity direction.[12] However, in liquid crystalline polymers, the combination of turbidity and large retardation would make this extremely difficult. A different approach is afforded by the principles of conoscopic observation, where an interference figure is generated by sending highly convergent light through the anisotropic sample, between crossed polarizers.[13] There is a correspondence between spatial location on the fringe pattern and the angle at which light passes through the sample; changes in retardation with propagation direction give rise to the multiple order fringes. Most importantly, off-normal light paths provide additional information that is not available in orthoscopic (normal) illumination. Conoscopy has been used extensively on quiescent or slightly distorted *monodomain* samples, most notably by Srinivasarao and Berry and co-workers.[14–18] In one important example, the sensitivity to the optical orientation angle in the shear plane has provided the means of confirming director

* To whom correspondence should be addressed.

• Abstract published in *Advance ACS Abstracts*, December 1, 1993.

0024-9297/94/2227-0483$04.50/0

tumbling in several systems.[15,18,19]

In this paper, we apply the principle of conoscopy by systematically changing the angle at which light propagates through a shear flow field and monitoring the corresponding changes in retardation. The application of this principle to textured PLC solutions is somewhat delicate. For instance, Srinivasarao and Berry report that when a shear-deformed monodomain ultimately degrades due to defect formation, the conoscopic pattern immediately vanishes.[15] However, the results of our previous work indicate that at a macroscopic level, the optical properties of a textured PLC may indeed be represented by eq 1. Provided that the texture length scales are much smaller than the optical volume and flow dimensions, it is reasonable that the sample would exhibit bulk optical anisotropy that is characteristic of the molecular orientation averaged over the polydomain texture. While there are some recognizable effects of the optically heterogeneous texture, the basic behavior observed in the spectrographic technique is that of a birefringent material.[10] In the context of the present work, the fringes visualized in Figure 4 illustrate again that the sample may be well represented as a birefringent material. We are therefore quite confident that the refractive index tensor as measured in this work does provide a qualitatively correct picture of the average orientation state in the sheared liquid crystalline polymer solution.

2. Predictions of Orientation State

The use of flow birefringence as a probe of molecular orientation in liquid crystalline polymer solutions relies on a connection between the refractive index tensor and the orientation probability distribution function. Provided the degree of optical anisotropy is not too large, there is a direct proportionality between the anisotropic part of the refractive index tensor and the order parameter tensor, **S**, essentially the second moment tensor of the orientation distribution function. In textured media, it must also be understood that the experimentally measured birefringence will reflect the orientation at both the molecular and mesoscopic (texture) levels. See ref 10 for a discussion of these issues in the context of our earlier work.

Various theories have been advanced to describe the rheological behavior of liquid crystalline polymers. In recent years, the Doi molecular model[20] has been shown to provide great insights into nonlinear viscoelastic effects such as the transition from tumbling at low shear rates to flow alignment at high shear rates,[21-24] and associated changes in the sign of normal stress differences.[25] Continuing the direction of our previous work, here we discuss predictions of the Doi model based on calculations by Larson.[24] Reference 10 includes the predictions for anisotropy in the order parameter tensor, $S_{11} - S_{33}$, of relevance to measurements of Δ_3. To summarize, tumbling at low shear rates results in a reduction in orientation to about 80% of the monodomain value. As shear rate is increased through the wagging and into the flow alignment regime, the orientation increases steadily, but remains below the monodomain value even at high rates.

Figure 1 shows Doi model predictions for $\chi = (1/2) \times \tan^{-1}[2S_{12}/(S_{11} - S_{22})]$ and $\Delta_2/\Delta_1 = (S_{22} - S_{33})/(S_{11} - S_{22})$ [these results were kindly provided by Dr. Larson]. In the tumbling and wagging regimes, time averages are taken over the periodic response; this procedure has been shown to result in rheological predictions which are reasonable, and it may be taken as a first approximation to compensate for the effect of a distribution of domain orientations in a textured material. At low shear rates, χ must tend toward zero, a consequence of time averaging the symmetric unperturbed tumbling orbit. At higher shear rates, χ becomes first positive and then undergoes two sign changes with increasing shear rate, reminiscent of sign changes in the normal stresses. This similarity is expected, given the physical interpretation of negative normal stresses discussed by Marrucci and Maffettone.[21] At all shears rates, the average molecular orientation is predicted to be quite close to the flow direction. Figure 1b shows that, at high shear rates, Δ_2/Δ_1 is very small. Since the orientation angle is quite close to zero, this implies that the order parameter tensor is approximately uniaxial in the high shear rate, flow aligning regime. Conversely, at low shear rates, this ratio is sizable and positive, indicating a relatively higher probability of finding molecules oriented along the gradient (2) direction than along the vorticity (3) direction. It should be noted that this prediction depends critically on the fact that only in-plane director orientations are included in these calculations;[24] the time average of a single, in-plane orbit leads naturally to this result. In textured materials, one expects contributions from domains oriented away from the flow direction, as well.

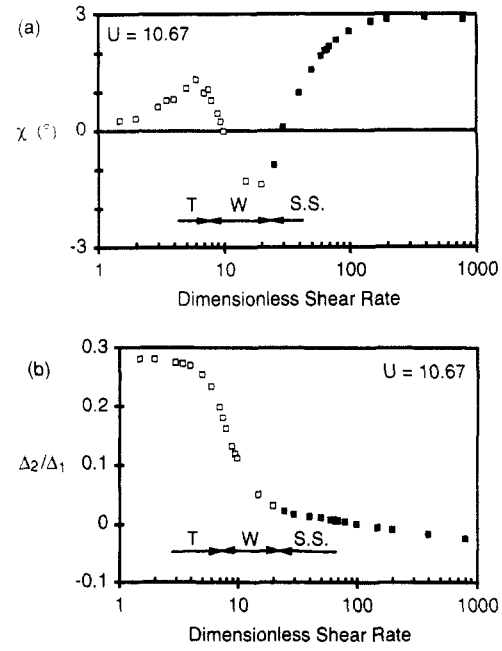

Figure 1. Orientation predictions of the Doi molecular model, with Onsager potential strength $U = 10.67$ (calculations of Larson[24]): (a) orientation angle, χ, vs dimensionless shear rate; (b) Δ_2/Δ_1 vs dimensionless shear rate. Regimes of tumbling (T), wagging (W), and steady state (SS) are indicated. Open symbols represent time averages.

In the linear, tumbling limit, Larson and Doi have proposed a model that describes textured polymer liquid crystals in terms of a distribution of domain orientations.[26] They argue that the dynamics of an individual domain will follow the linear Leslie–Ericksen theory, and then formally average the response over the domain distribution function, using a phenomenological form for the averaged influence of distortional elasticity. The resulting model is formulated in terms of a mesoscopic order parameter tensor, $\bar{\mathbf{S}}$, representing the second moment of the *domain* orientation distribution function. Since the model seeks to describe the linear limit, no change in orientation is expected at the molecular level, so that the average orientation state (and hence refractive index tensor) is determined solely by $\bar{\mathbf{S}}$.

The Larson and Doi model predicts an average orientation state which is independent of shear rate in the linear regime, while a length scale associated with the texture is

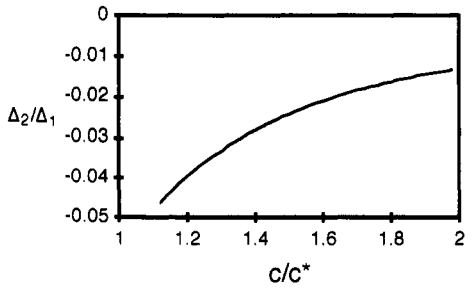

Figure 2. Steady state Larson–Doi polydomain model predictions of Δ_2/Δ_1 as a function of dimensionless concentration.

refined with increasing shear rate. Our previous results on PBG are consistent with these predictions,[10] although studies on hydroxypropylcellulose show changing orientation at all shear rates.[8,27] The orientation state is determined by two variables: c/c^*, a dimensionless concentration (this determines the Leslie coefficients from the linearized Doi model[28]) and an elastic parameter, ϵ. Reference 10 shows predictions for $\bar{S}_{11} - \bar{S}_{33}$ and χ. For reasonable parameter ranges, the Larson–Doi model predicts a value of Δ_3 in the range of 80–90% of the monodomain birefringence and a positive orientation angle of a few degrees. The steady state value of Δ_2/Δ_1 predicted by the Larson–Doi model depends only on the Leslie coefficients, α_i, according to

$$\frac{\Delta_2}{\Delta_1} = \frac{\alpha_3}{\alpha_2 - \alpha_3} \tag{3}$$

Since the Leslie coefficients are determined solely by concentration, this means that this quantity is independent of the elasticity parameter, ϵ. Figure 2 shows the model predictions for Δ_2/Δ_1 as a function of concentration. For reasonable values of the concentration, Δ_2/Δ_1 is much smaller in magnitude than the low shear rate predictions of Figure 1b and is negative. Thus, the formal inclusion of out-of-plane orbits in the Larson–Doi model does have a major impact on the predicted transverse anisotropy (Δ_2).

One prediction shared by the Larson–Doi model and time-averaged Doi model at low shear rates is the prediction of a relatively high degree of molecular orientation, reflected in the predictions of Δ_3. The fact that the experimentally observed orientation is only 50–60% of the monodomain value in the tumbling limit is a considerable discrepancy[10] and one of our present motivations for obtaining more complete information about the orientation state. In addition, full characterization of **n** provides a basis for a more detailed test of these models than has been possible using only a single projection of the orientation state.

3. Experimental Methods

3.1. Materials. Experiments were performed on two solutions of poly(γ-benzyl glutamate) in *m*-cresol, at concentrations of 13.5 and 20.0 wt %. The 13.5% solution used the single optical isomer PBDG, purchased from Sigma (Lot 110H5531), with a reported molecular weight of 298 000. The 20% solution used a racemic mixture (denoted PBG) formed by mixing the PBDG sample described above with an equal mass of PBLG (Sigma Lot 60h5512) of similar molecular weight (reported as 310 000). Solvent *m*-cresol was also purchased from Sigma; all materials were used as received. Solutions were mixed by weight, allowing several weeks for dissolution of the polymer. The 20% solution was used in our earlier work; the 13.5% solution is very similar to another sample in the same study.[10,11]

3.2. Optical Technique. Figure 3 shows a schematic illustration of the flow and optical geometry used in this work.

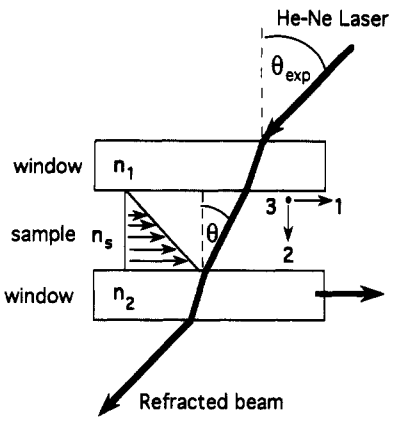

Figure 3. Schematic illustration of angled light configuration.

The flow cell consists of circular optical windows separated by a distance d (1.94 mm in the present work). When the light path is displaced away from the axis of rotation of the lower window, a shear flow is observed that is approximately homogeneous on the length scale of the light beam used (approximately 1 mm). In this experiment, optical anisotropy is measured as a function of the angle at which light passes through the sheared PLC, θ. The birefringence may be calculated by a suitable coordinate frame rotation of the refractive index tensor, leading to

$$\Delta n(\theta) = \Delta_3 \cos^2\theta + \Delta_2 \sin^2\theta + (\Delta_3 - \Delta_2) \tan 2\chi \sin\theta \cos\theta \tag{4}$$

The birefringence is seen to depend on three independent optical properties, which we have taken here to be Δ_3, Δ_2, and χ.

Changes in retardation with angle are monitored using a crossed and parallel polarizer arrangement similar to that employed in the spectrographic technique[10] and used by Mattoussi and coworkers.[16,17] The polarizers are oriented at 45° with respect to the flow direction and are either crossed or parallel to one another. Since light suffers polarization and intensity changes as it is refracted through the air–glass and glass–solution interfaces, it is necessary to account for these effects in the optical analysis. This results in the following expressions for light intensity transmitted between crossed ($\perp$) and parallel ($\parallel$) polarizers:

$$I^{\perp}(\theta_{exp}) = I_0\left[T_1 \sin^2\left(\frac{\pi\Delta n(\theta)d}{\lambda\cos\theta}\right) + T_2 \cos^2\left(\frac{\pi\Delta n(\theta)d}{\lambda\cos\theta}\right)\right] \tag{5a}$$

$$I^{\parallel}(\theta_{exp}) = I_0\left[T_1 \cos^2\left(\frac{\pi\Delta n(\theta)d}{\lambda\cos\theta}\right) + T_2 \sin^2\left(\frac{\pi\Delta n(\theta)d}{\lambda\cos\theta}\right)\right] \tag{5b}$$

Here I_0 is the incident light intensity, λ is the wavelength of light used, and θ_{exp} is the angle of light propagation measured experimentally, external to the flow cell (see Figure 3). Snell's law is used to relate θ_{exp} to θ, the propagation angle within the PLC, allowing eq 4 to be used to calculate $\Delta n(\theta)$. T_1 and T_2 are correction factors for refraction effects, expressed in terms of Fresnel coefficients.[29] They depend on the refractive indices of the windows ($n_1 = 1.515\,09$ and $n_2 = 1.457\,02$ in our cell) and the solution ($n_s = 1.543$) and the light propagation angle. The major effect of refraction is a gradual reduction in transmitted intensity as the angle is increased. T_1 is generally much larger than T_2, so that the basic behavior is an out-of-phase oscillation in $I^{\perp}$ and $I^{\parallel}$ as the retardation changes with angle.

This analysis neglects higher order effects associated with the fact that the ordinary and extraordinary rays are refracted slightly differently and thus follow different paths through the sample. In these materials, the birefringence is substantially smaller in magnitude than the individual refractive indices, so that we assume that both rays follow essentially the same path through the sample. A similar assumption was made by Mattoussi et al.[17] There is also ambiguity about the precise value to be used for n_s in accounting for refraction effects, since liquid crystals are characterized by *two* refractive indices. An Abbe refractometer was used with HeNe laser illumination and a polarizer to approximately determine the refractive index ranges which characterize these solutions;[31] the values of 1.543 is an average, used in the analysis of data for both solutions. Since n_s determines

θ for a given θ_{exp}, the assumed value does affect the analysis of the data; however, using a range of n_s values from 1.54 to 1.55 in the analysis procedure had a negligible impact on the results.

3.3. Experimental Procedures. The optical train consists of a HeNe laser, two polarizers, and a detector mounted on a short optical rail, which is in turn mounted on a large precision rotation stage. The flow cell is located such that rotation of the light beam results in no change in the position at which the beam passes through the flow cell. The flow cell has been machined to admit a wide range of incident light angle; typically experiments are performed over the range $-55° < \theta_{exp} < +50°$. As the angle is changed, the beam exiting the flow cell is displaced due to refraction effects. To compensate, the detector is occasionally shifted laterally to keep the beam centered on the detector surface. This procedure is imperfect and results in additional scatter in the data; however, the large scale features upon which the analysis is based are unaffected.

The flow cell is driven by a computerized microstepping motor of high precision (Computer 4000 indexer system). In steady flow measurements, trigger signals from the indexer are used to coordinate computerized acquisition of intensity readings, such that measurements are always made at the same position of the flow cell, one measurement per revolution. This is necessary owing to a small ($\approx$5%) variation in sample thickness as the flow cell is rotated.[10,11] The sample is always presheared for at least 200 strain units prior to initiating data acquisition in steady experiments, or prior to flow cessation in relaxation experiments. The total time to complete both crossed and parallel angular scans is around 15–20 min for relaxation measurements; in steady experiments, this time could be much longer depending on the shear rate.

Results of a single "experiment" are scans of transmitted intensity as a function of angle, for both parallel and crossed polarizers. The data are analyzed by fitting the observed fringe patterns to eqs 4 and 5. For each experiment, a complementary measurement of Δ_3 is taken at the same flow cell position using the spectrographic technique; see ref 10 for a detailed discussion of the methods used. This value of Δ_3 is used as a starting point in the fitting procedure. Δ_3 determines the levels of the crossed and parallel intensities at $\theta_{exp} = 0$. For highly birefringent materials, there are multiple orders of retardation present and, consequently, many values of Δ_3 that could match the $\theta_{exp} = 0$ intensities; the spectrographic technique eliminates this ambiguity. It is sometimes necessary to adjust the value of Δ_3 slightly from the spectrographic value to exactly fit the behavior at $\theta_{exp} = 0$. Comparisons of the spectrographic data and the values used in the fitting procedures are shown in Figure 5a below. Once Δ_3 is fixed, χ is determined by fitting the degree of asymmetry in the fringe pattern, while Δ_2 is adjusted by fitting the rate at which fringes appear as $|\theta_{exp}|$ is increased. While the measurement of χ is very direct, the value of Δ_2 is extremely sensitive to the assumed value of Δ_3. Thus, it is important that care be taken to determine Δ_3 accurately before attempting to adjust Δ_2. In this respect, again, it is useful to have an independent accurate value of Δ_3 from the spectrographic technique. The uncertainty associated with determination of Δ_2 is discussed in the next section.

3.4. Illustration of Technique. Figure 4 shows typical raw intensity data transmitted between crossed and parallel polarizers as a function of the external angle made by the light path relative to the flow cell, for steady shear flow of the 13.5% solution. The data exhibit the maxima and minima expected for what is essentially a cross section of a conoscopic fringe pattern. For an ideal birefringent material, the fringes would be completely extinguished at certain angles. However, as discussed at length in our earlier paper,[10] the variability in averaged optical properties across the light path associated with the texture results in a depolarization effect due to the mixing of various polarization states in the light leaving the sample. Thus, true extinction conditions do not occur. Similar optical effects have been described in the context of randomly oriented textured block copolymers.[31,32] In our spectrographic experiments, these effects were characterized by an amplitude, A, equal to 1 for an ideal retarder.[10] Note that in Figure 4 the amplitude of the oscillatory response is reduced to a greater extent at the lower shear rate (a) than at the higher shear rate (b). This is entirely consistent

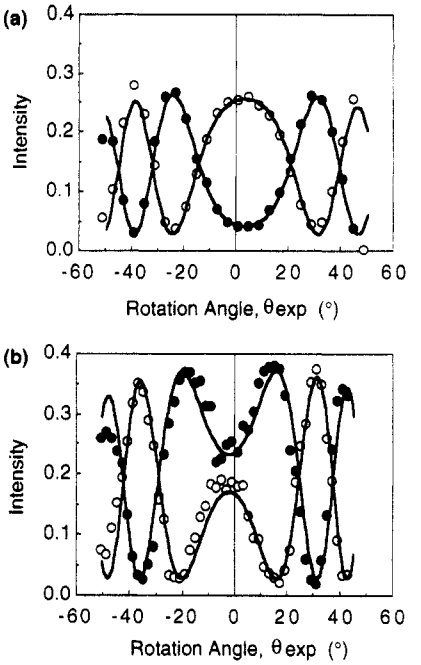

Figure 4. Intensity transmitted between crossed (●) and parallel (○) polarizers, as a function of light path angle for a 13.5% solution of PBDG: (a) shear rate = 0.35 s^{-1}, $\Delta_3 = 0.002253$, $\chi = 1.1°$, $\Delta_2/\Delta_1 = -0.128$; (b) shear rate = 30 s^{-1}, $\Delta_3 = 0.003469$, $\chi = -0.8°$, $\Delta_2/\Delta_1 = 0.088$. Note the change in sign of χ with increasing shear rate. Lines are drawn according to eqs 4 and 5.

with the steady state behavior of A (see Figure 7 in ref 10). Despite the presence of these depolarization effects, the oscillatory fringe pattern is unmistakable, and may be well fit by eqs 5 (note that the solid lines have had their amplitude adjusted to account for the depolarization effects). In the 13.5% solution, there is an intermediate shear rate range where depolarization effects become sufficiently severe that no clear fringe pattern could be observed. A similar regime of strong depolarization was also seen with the spectrographic technique, occurring in a shear rate range where "wagging" is expected on the basis of Doi model predictions.[24] A striking striped texture is observed in optical microscopy of sheared PBG solutions in this regime.[3]

The heading to Figure 4 reports the value of the refractive index tensor components used to generate the calculated curves. Comparing parts a and b, the higher shear rate is characterized by a higher average degree of orientation, resulting in a greater number of fringes as the angle is scanned. In addition, it is qualitatively clear that the sign of the orientation angle has changed with the increase in shear rate. A small degree of rotation ($|\chi| < 2°$) of the average orientation up or down from the flow direction results in an easily discernable shift in the interference fringe (particularly at large $|\theta_{exp}|$), so that small values of χ may be quite accurately measured. Given the small observed orientation angle, a slight misalignment of the optics with respect to the flow cell can possibly result in errors (the optics were assembled separately for each block of steady state or relaxation experiments). To check against this possibility, experiments were conducted in which the flow cell was rotated in both forward and backward directions, at several shear rates for both solutions. In all cases, changing the flow direction changed the apparent sign of χ (as it should), but there was a small systematic error in its magnitude (which should be equal for the opposite directions). From these experiments, correction factors of -0.2 and $-0.1°$ were determined to be necessary for the steady state experiments using 13.5% and 20% solutions, respectively. Relaxation experiments were also conducted using both forward and backward flow cell motion. In these experiments, a correction factor of $-0.15°$ was required for the 30-s^{-1} experiments, while no correction factor was required for the 1-s^{-1} relaxation experiments. The data shown in Figures 5b and 6b have been corrected accordingly.

Table 1 illustrates the sensitivity of the determination of Δ_2 to the assumed value of Δ_3, discussed in the preceding section. The Δ_3 values used in this table cover the range for which a

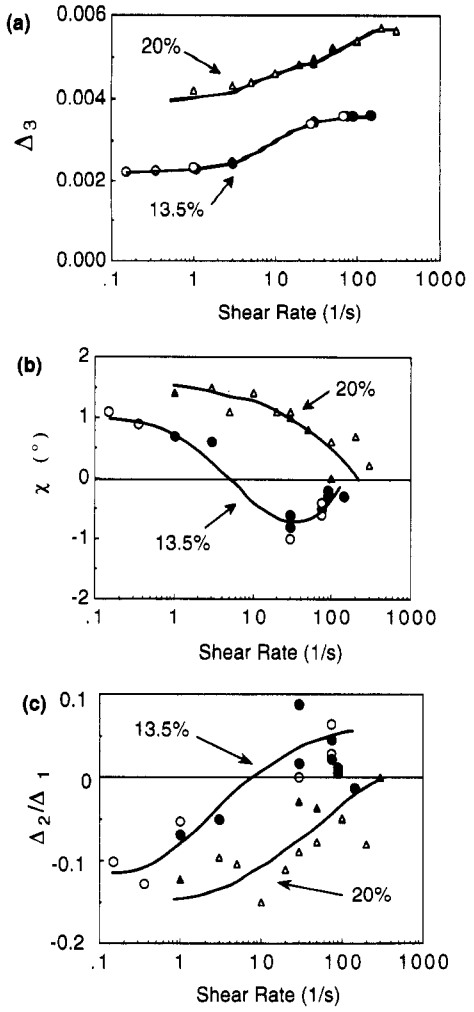

Figure 5. Steady state behavior of the refractive index tensor in PBG solutions. (a) Δ_3 vs shear rate. Solid curves give spectrographic results, while symbols give values used in analyzing angled light experimental data. (b) Orientation angle, χ, vs shear rate. (c) Δ_2/Δ_1 vs shear rate. Filled symbols are data from experiments conducted with the flow cell rotating in the opposite direction. In (b) and (c), lines are drawn to aid the eye.

Table 1. Sensitivity of Δ_2/Δ_1 to Assumed Δ_3 (Data from Figure 4a, 13.5% Solution, 0.35 s^{-1})

assumed Δ_3	χ (deg)	Δ_2/Δ_1
0.002 243	1.1	−0.111
0.002 248	1.1	−0.118
0.002 253	1.1	**−0.128**
0.002 258	1.1	−0.141
0.002 263	1.1	−0.153

reasonable fit of the equations to the conoscopic patterns of Figure 4a is obtained; the best fit to the curves is achieved using the values in boldface. The variation in Δ_2/Δ_1 seen in this table may be taken as typical of the uncertainty in the reported values of this quantity. Note that the value of the orientation angle is unaffected by the assumed Δ_3.

4. Results and Discussion

4.1. Steady Shear Flow. Figure 5 summarizes our measurements of the full refractive index tensor as a function of steady shear rate for both solutions studied. Figure 5a shows measurements of Δ_3 obtained using the spectrographic technique. These data follow the trends seen in our earlier work.[10] There is a low shear rate plateau in the birefringence associated with the linear tumbling regime. At intermediate shear rates, there is a transition to a higher orientation state, reaching another plateau at higher shear rates. On the basis of comparisons with transitions in normal stresses, we have attributed this increase in birefringence to the transition from tumbling to flow alignment with increasing shear rate, as predicted by the Doi model. The transition is shifted to higher shear rates with increased concentration. This is consistent with other observations; in particular, the concentration dependence of normal stress transitions has been shown by Magda and co-workers to be well predicted by the Doi model.[25]

Parts b and c of Figure 5 show the remaining two independent quantities that fully determine the refractive index tensor; here we present data for the optical orientation angle in the 1–2 plane and the ratio of the second to the first normal optical difference. In the 13.5% solution, the orientation angle is seen to have a small positive value at low shear rates. As shear rate is increased, the orientation angle changes sign, as is evident from the raw data in Figure 4. At the highest shear rates for which measurements were possible, there are signs that χ is tending once again toward positive values. The 20% solution has a positive χ for all shear rates studied, although it is steadily decreasing with increasing shear rate. In Figure 5c, the second normal optical difference is seen to be negative for both solutions at low shear rates, with a magnitude in the range of 10–15% of Δ_1. As the shear rate increases, both solutions show an increasing Δ_2. In the 13.5% solution, Δ_2 charges sign but is smaller in magnitude than at low shear rates. The 20% solution seems to exhibit similar behavior, but shifted toward higher shear rates, so that no sign change in Δ_2 is observed.

The behavior in Figure 5 may be compared with the predictions of molecular and mesoscopic models in section 2. In our previous work, we noted that the orientation in the 1–3 plane (Δ_3) is substantially overpredicted by tumbling models in the low shear rate regime.[10] One possible explanation would be that the average orientation was in fact high, but that the optical axis was rotated away from the 1–3 plane (i.e., large χ), leading to the lower than expected birefringence. The data in Figure 5b clearly show the failings of this explanation, in that χ is within 2 deg of the flow direction at all shear rates. Thus, the lower than expected Δ_3 unambiguously indicates that the average order parameter under flow is substantially lower than in a quiescent monodomain.

On the basis of direct microscopic observations by Larson and Mead at extremely low Ericksen number,[2] we hypothesized that another explanation for the low orientation could be a systematic misalignment of the director in the 1–3 plane away from the flow direction (i.e. *toward* the vorticity axis).[10] Symmetry dictates (and Larson and Mead observe) that the misaligned domains would be equally distributed on either side of the flow direction, so that *on average*, the optical anisotropy remains orientated along the flow direction in the 1–3 plane. If this explanation is correct, there should be a higher than expected probability of finding molecules oriented along the vorticity axis, due to the systematic alignment away from the flow direction. Indeed, at low shear rates, Δ_2 is negative, indicating a higher probability of finding rods in the 3-direction than the 2-direction. While this is qualitatively consistent with the predictions of the Larson–Doi polydomain model (Figure 2), the magnitude of Δ_2/Δ_1 in the low shear rate regime is substantially higher than the model predictions. These data thus appear to be consistent with the hypothesis that the tumbling regime in PBG solutions is characterized by a significant misalignment of domains out of the shear plane. However, recent neutron scattering data by Dadmun and Han[33] do not support the existence of discrete populations of misaligned domains in PBG

solutions, but rather indicate a unimodal distribution of molecular orientation around the flow direction at all shear rates, in agreement with X-ray scattering data on several other systems.[6-8] It is possible that the systematic misalignment observed by Larson and Mead does not persist into higher Ericksen number regimes where the texture length scale is substantially refined and polarimetric determination of the orientation within a single domain is impossible.[3]

A useful alternative representation of the orientation state at low shear rates is the second moment tensor for the domain distribution function, expressed in terms of Larson and Doi's mesoscopic order parameter as

$$\langle \mathbf{nn} \rangle = \bar{\mathbf{S}} + \frac{1}{3}\mathbf{I} \tag{6}$$

Assuming the orientation state at the molecular level is not perturbed by the shear flow at low rates, all reduction of orientation in the linear limit may be attributed to the distribution of domain orientations. In our previous work, we noted that the low shear rate plateau of Δ_3 is in the range of 50–60% of the monodomain value.[10] Taking an average value yields the condition $\bar{S}_{11} - \bar{S}_{33} = 0.55$. This may be combined with measurements from the present study to construct an experimentally determined second moment tensor.

For comparison, a uniformly oriented monodomain (along the 1-axis), has $\langle \mathbf{nn} \rangle$ given by

$$\langle \mathbf{nn} \rangle_{\text{monodomain}} = \begin{bmatrix} 1 & 0 & 0 \\ 0 & 0 & 0 \\ 0 & 0 & 0 \end{bmatrix} \tag{7}$$

Taking typical values of $c/c^* = 1.122$ and $\epsilon = 0.03$, the Larson–Doi model prediction is

$$\langle \mathbf{nn} \rangle_{\text{Larson-Doi}} = \begin{bmatrix} 0.866 & 0.048 & 0 \\ 0.048 & 0.048 & 0 \\ 0 & 0 & 0.085 \end{bmatrix} \tag{8}$$

Finally, using the values for 13.5% PBDG at a shear rate of 0.35 s^{-1} (data from Figure 4a), the experimentally determined second moment tensor is

$$\langle \mathbf{nn} \rangle_{\text{experiment}} = \begin{bmatrix} 0.727 & 0.010 & 0 \\ 0.010 & 0.096 & 0 \\ 0 & 0 & 0.177 \end{bmatrix} \tag{9}$$

Comparing these expressions, it is clear that the Larson–Doi model underpredicts the disruption of orientation associated with the tumbling shear flow of the textured PLC.[10] As expected from the earlier discussion of Δ_2/Δ_1 at low rates, the experiments indicate a substantially higher probability of finding rods along the vorticity (3) axis than the Larson–Doi model predicts. However, it is also noteworthy that the experimental results also show a higher degree of misalignment toward the 2-direction than predicted by the Larson–Doi model. Thus, the lower than predicted Δ_3 results from misalignment of domains not only *within* the 1–3 plane but also *out* of the 1–3 plane. Finally, we note that the orientation angles observed at low shear rates are somewhat smaller than the Larson–Doi predictions,[10] leading to a smaller off-diagonal element in $\langle \mathbf{nn} \rangle_{\text{experiment}}$.

As discussed in section 2, the Doi molecular model prediction of *positive* Δ_2 at low shear rates (Figure 1a) is an artifact of the fact that only an in-plane orbit was averaged in Larson's calculations. However, as the shear rate is increased into the nonlinear regime, we may compare our data with the predictions in Figure 1. The most striking predictions are sign changes in the orientation angle with increasing shear rate. The data in Figure 5b for the 13.5% solution seem to be in excellent qualitative agreement with the Doi model orientation angle predictions. In addition, in the flow alignment regime at high shear rates, the Doi model predicts that Δ_2 should be relatively small in magnitude, indicating that the average orientation state is roughly uniaxial. The small magnitude of Δ_2/Δ_1 observed at high shear rates in Figure 5c generally supports this prediction as well.

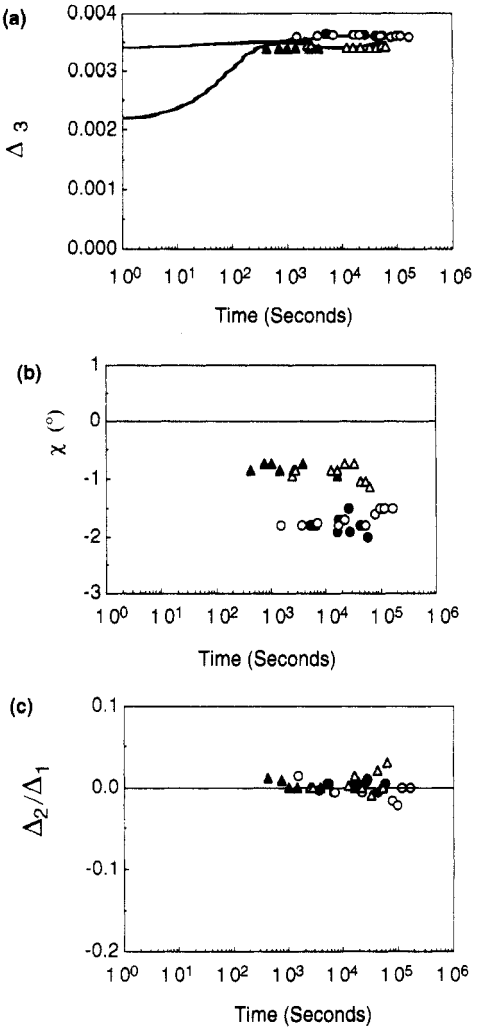

Figure 6. Relaxation in a 13.5% PBDG solution following shear flow (circles, 1 s^{-1}; triangles, 30 s^{-1}): (a) Δ_3 vs time, as measured by the spectrographic technique (solid lines), showing values used in analyzing angled light experimental data (symbols); (b) orientation angle, χ, vs time; (c) Δ_2/Δ_1 vs time. Filled symbols are data from an experiment conducted with the flow cell rotating in the opposite direction.

4.2. Relaxation Behavior. One of the striking results of our earlier work was the observation of a dramatic increase in orientation upon flow cessation in PBG solutions, to a value comparable to that of a defect-free monodomain.[11] This contrasted with earlier studies where decreasing orientation toward an isotropic structure was reported, in both PBG[34] and other systems.[6,35] While the time scale required for completion of one angular scan in the present technique is too long to study transient phenomena in real time, here we report the long-time structure that results following cessation of flow at two rates: 1 s^{-1}, within the low shear rate (tumbling) plateau, and 30 s^{-1}, in the high shear rate, flow alignment regime. Figure 6a shows the typical time evolution of Δ_3 following flow cessation in the 13.5% solution, as measured using the spectrographic technique. The sample relaxes to an extremely well-ordered condition. At 1 s^{-1}, there is a large

increase in Δ_3, due to the disruption of orientation during flow in the tumbling regime, while at 30 s^{-1}, the orientation stays roughly constant at a high value. We have shown how these changes in the orientation state result in a corresponding evolution in dynamic moduli following flow cessation.[11,36]

On longer time scales, the angled light experiment was used to measure χ and Δ_2/Δ_1. In Figure 6b, for a prior shear rate of 30 s^{-1} we find that the orientation angle appears to remain in the range −0.7 to −1°, characteristic of the value of χ under steady flow at this rate (see Figure 5b). However, for a prior shear rate of 1 s^{-1}, the long-time relaxed structure has a χ which is significantly negative. Comparison with Figure 5b shows that this magnitude of the orientation is in fact larger than that observed during flow at any shear rate. Since the prior shear rate for these experiments is in the low shear rate regime where χ is positive, this result also means that the orientation angle changes sign during the relaxation. Unfortunately, this process cannot be followed in real time using the techniques employed here. It is reasonable to expect that this rearrangement is driven by the substantial distortional elasticity expected in shear flows of tumbling PLCs at low rates.[26]

While the behavior of χ is very puzzling, Figure 6c shows that Δ_2 is equal to zero for the long-time, high orientation state, indicating that this condition is characterized by a uniaxial average orientation state irrespective of the previously applied shear rate. This might be expected, since the degree of orientation in this state is comparable to that in a uniformly oriented monodomain.[11] After 24–36 h following the cessation of flow, the coonoscopic pattern produced by the angled light technique degraded in quality and could not be well described by eqs 5. This perhaps reflects the eventual formation of a cholesteric phase in this solution of a single optical isomer, PBDG.

5. Conclusions

We have reported the first measurements of the full refractive index tensor in sheared polymer liquid crystal solutions. In PBG solutions under steady shear flow at low rates, the average molecular orientation angle is small and positive, while the average orientation state is biaxial, with an enhanced probability of finding rods oriented along the vorticity direction relative to the shear gradient direction. The Larson–Doi model qualitatively captures these features but underpredicts the degree of misalignment both within and out of the 1–3 plane. As the shear rate is increased, a sign change is observed in the average orientation angle, consistent with predictions of the nonlinear Doi molecular model. In addition, the high shear rate, flow aligning regime is characterized by a roughly uniaxial average orientation distribution function. The nonlinear transitions appear to be shifted to higher shear rates with increased concentration.

Long after cessation of shear flow, PBG relaxes to a highly oriented condition, with a uniaxial distribution of molecular orientation. While the orientation angle in the shear plane appears to remain constant following cessation of flow at high rates, it changes from positive to negative values during the relaxation from flow at low rates. The origin of this behavior is unknown.

Acknowledgment. We gratefully acknowledge financial support from the National Science Foundation, under Award No. CTS-9109898, and through the MRL program at the Materials Research Center of Northwestern University, under Award No. DMR-9120521. In addition, we thank Dr. R. Larson for providing the calculation results presented in Figure 1.

References and Notes

(1) Gleeson, J. T.; Larson, R. G.; Mead, D. W.; Kiss, G.; Cladis, P. E. *Liq. Cryst.* **1992**, *11*, 341.
(2) Larson, R. G.; Mead, D. W. *Liq. Cryst.* **1992**, *12*, 751.
(3) Larson, R. G.; Mead, D. W. *Liq. Cryst.* **1993**, *15*, 151.
(4) Vermant, J.; Moldenaers, P.; Picken, S. J.; Mewis, J. Submitted for publication to *J. Non-Newtonian Fluid Mech.*
(5) Picken, S. J.; Moldenaers, P.; Berghmans, S.; Mewis, J. *Macromolecules* **1992**, *25*, 4759.
(6) Picken, S. J.; Aerts, J.; Doppert, H. L.; Reuvers, A. J.; Northolt, M. G.; *Macromolecules* **1991**, *24*, 1366.
(7) Odell, J. A.; Ungar, G.; Feijoo, J. L. *J. Polym. Sci. Part B: Polym. Phys.* **1993**, *31*, 141.
(8) Keates, P.; Mitchell, G. R.; Peuvrel-Disdier, E.; Navard, P. *Polymer* **1993**, *34*, 1316.
(9) Chow, A.; Hamlin, R. D.; Ylitalo, C. *Macromolecules* **1992**, *25*, 7135.
(10) Hongladarom, K.; Burghardt, W. R.; Baek, S. G.; Cementwala, S.; Magda, J. J. *Macromolecules* **1993**, *26*, 772.
(11) Hongladarom, K.; Burghardt, W. R. *Macromolecules* **1993**, *26*, 785.
(12) See, for instance: Janeschitz-Kriegl, H. *Adv. Polym. Sci.* **1969**, *6*, 170.
(13) Gay, P. *An Introduction to Crystal Optics*; Longmans: London, 1967.
(14) Berry, G. C.; Srinivasarao, M. *J. Stat. Phys.* **1991**, *62*, 1041.
(15) Srinivasarao, M.; Berry, G. C. *J. Rheol.* **1991**, *35*, 379.
(16) Mattoussi, H.; Srinivasarao, M.; Kaatz, P. G.; Berry, G. C. *Mol. Cryst. Liq. Cryst.* **1992**, *223*, 69.
(17) Mattoussi, H.; Srinivasarao, M.; Kaatz, P. G.; Berry, G. C. *Macromolecules* **1992**, *25*, 2860.
(18) Srinivasarao, M.; Garay, R. O.; Winter, H. H.; Stein, R. S. *Mol. Cryst. Liq. Cryst.* **1992**, *223*, 29.
(19) Burghardt, W. R.; Fuller, G. G. *Macromolecules* **1991**, *24*, 2546.
(20) Doi, M. *J. Polym. Sci., Polym. Phys. Ed.* **1981**, *19*, 229.
(21) Marrucci, G.; Maffettone, P. L. *Macromolecules* **1989**, *22*, 4076.
(22) Marrucci, G.; Maffettone, P. L. *J. Rheol.* **1990**, *34*, 1217.
(23) Marrucci, G.; Maffettone, P. L. *J. Rheol.* **1990**, *34*, 1231.
(24) Larson, R. G. *Macromolecules* **1990**, *23*, 3983.
(25) Magda, J. J.; Baek, S.-G.; DeVries, K. L.; Larson, R. G. *Macromolecules* **1991**, *24*, 4460.
(26) Larson, R. G.; Doi, M. *J. Rheol.* **1991**, *35*, 539.
(27) Burghardt, W. R.; Hongladarom, K.; Secakusuma, V. To be submitted to *J. Rheol.*
(28) Kuzuu, N.; Doi, M. *J. Phys. Soc. Jpn.* **1984**, *53*, 1031.
(29) Azzam, R. M. A.; Bashara, N. M. *Ellipsometry and Polarized Light*; Elsevier: Amsterdam, 1987.
(30) DuPre, D. P.; Lin, F. M. *Mol. Cryst. Liq. Cryst.* **1981**, *75*, 217.
(31) Amundson, K.; Helfand, E.; Patel, S. S.; Quan, X.; Smith, S. D. *Macromolecules* **1992**, *25*, 1935.
(32) Balsara, N. P.; Garetz, B. A.; Dai, H. J. *Macromolecules* **1992**, *25*, 6072.
(33) Dadmun, M. D.; Han, C. C. *Polym. Prepr. (Am. Chem. Soc., Div. Polym. Chem.)* **1993**, *2*, 733.
(34) Asada, T.; Onogi, S.; Yanase, H. *Polym. Eng. Sci.* **1984**, *24*, 355.
(35) Onogi, S.; White, J. L., Fellers, J. F. *J. Non-Newtonian Fluid Mech.* **1980**, *7*, 121.
(36) Moldenaers, P.; Mewis, J. *J. Rheol.* **1993**, *37*, 367.